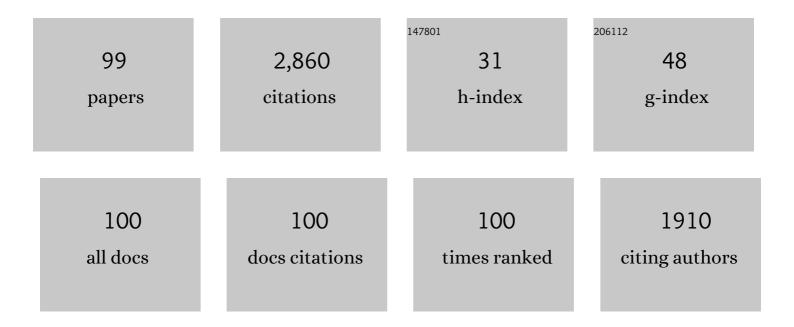
Xia Liao

List of Publications by Year in descending order

Source: https://exaly.com/author-pdf/4355555/publications.pdf Version: 2024-02-01



YIA LIAO

#	Article	IF	CITATIONS
1	Light-weight and flexible silicone rubber/MWCNTs/Fe3O4 nanocomposite foams for efficient electromagnetic interference shielding and microwave absorption. Composites Science and Technology, 2019, 181, 107670.	7.8	173
2	Flexible thermoplastic polyurethane/reduced graphene oxide composite foams for electromagnetic interference shielding with high absorption characteristic. Composites Part A: Applied Science and Manufacturing, 2019, 123, 310-319.	7.6	141
3	Gradient structure design of lightweight and flexible silicone rubber nanocomposite foam for efficient electromagnetic interference shielding. Chemical Engineering Journal, 2020, 390, 124589.	12.7	124
4	Facile and Green Method To Structure Ultralow-Threshold and Lightweight Polystyrene/MWCNT Composites with Segregated Conductive Networks for Efficient Electromagnetic Interference Shielding. ACS Sustainable Chemistry and Engineering, 2019, 7, 9904-9915.	6.7	101
5	Frequency-selective and tunable electromagnetic shielding effectiveness via the sandwich structure of silicone rubber/graphene composite. Composites Science and Technology, 2019, 184, 107847.	7.8	80
6	Heterogeneous silicon rubber composite foam with gradient porous structure for highly absorbed ultra-efficient electromagnetic interference shielding. Composites Science and Technology, 2021, 206, 108663.	7.8	74
7	Effect of Unexpected CO ₂ 's Phase Transition on the High-Pressure Differential Scanning Calorimetry Performance of Various Polymers. ACS Sustainable Chemistry and Engineering, 2016, 4, 1810-1818.	6.7	69
8	Control of the cell structure of microcellular silicone rubber/nanographite foam for enhanced mechanical performance. Materials and Design, 2017, 133, 288-298.	7.0	68
9	Carbon dioxideâ€induced crystallization in poly(<scp>L</scp> â€lactic acid) and its effect on foam morphologies. Polymer International, 2010, 59, 1709-1718.	3.1	65
10	Polymer–CO2 systems exhibiting retrograde behavior and formation of nanofoams. Polymer International, 2007, 56, 67-73.	3.1	62
11	Fabrication of lightweight and flexible silicon rubber foams with ultra-efficient electromagnetic interference shielding and adjustable low reflectivity. Journal of Materials Chemistry C, 2020, 8, 147-157.	5.5	60
12	Layered Open Pore Poly(l-lactic acid) Nanomorphology. Biomacromolecules, 2006, 7, 2937-2941.	5.4	56
13	Crystals <i>in Situ</i> Induced by Supercritical CO ₂ as Bubble Nucleation Sites on Spherulitic PLLA Foam Structure Controlling. Industrial & Engineering Chemistry Research, 2017, 56, 11111-11124.	3.7	56
14	The effects of viscoelastic properties on the cellular morphology of silicone rubber foams generated by supercritical carbon dioxide. RSC Advances, 2015, 5, 106981-106988.	3.6	53
15	Unique interfacial and confined porous morphology of PLA/PS blends in supercritical carbon dioxide. RSC Advances, 2014, 4, 45109-45117.	3.6	50
16	Facile Fabrication of Lightweight Shape Memory Thermoplastic Polyurethane/Polylactide Foams by Supercritical Carbon Dioxide Foaming. Industrial & Engineering Chemistry Research, 2020, 59, 7611-7623.	3.7	50
17	An Ultraviolet-Induced Reactive Extrusion To Control Chain Scission and Long-Chain Branching Reactions of Polylactide. Industrial & Engineering Chemistry Research, 2016, 55, 597-605.	3.7	49
18	Mechanical–Microstructure Relationship and Cellular Failure Mechanism of Silicone Rubber Foam by the Cell Microstructure Designed in Supercritical CO ₂ . Journal of Physical Chemistry C, 2019, 123, 26947-26956.	3.1	49

Χια Liao

#	Article	IF	CITATIONS
19	A promising strategy for efficient electromagnetic interference shielding by designing a porous double-percolated structure in MWCNT/polymer-based composites. Composites Part A: Applied Science and Manufacturing, 2020, 138, 106059.	7.6	49
20	A two-step process for the preparation of thermoplastic polyurethane/graphene aerogel composite foams with multi-stage networks for electromagnetic shielding. Composites Communications, 2020, 21, 100416.	6.3	48
21	The sorption behaviors in PLLA-CO2 system and its effect on foam morphology. Journal of Polymer Research, 2012, 19, 1.	2.4	46
22	Carbon nanotube-reinforced silicone rubber nanocomposites and the foaming behavior in supercritical carbon dioxide. Journal of Supercritical Fluids, 2018, 141, 78-87.	3.2	44
23	Introduction of a long-chain branching structure by ultraviolet-induced reactive extrusion to improve cell morphology and processing properties of polylactide foam. RSC Advances, 2017, 7, 6266-6277.	3.6	42
24	Creating orientated cellular structure in thermoplastic polyurethane through strong interfacial shear interaction and supercritical carbon dioxide foaming for largely improving the foam compression performance. Journal of Supercritical Fluids, 2019, 153, 104577.	3.2	38
25	Crystallization and morphological transition of poly(<scp>l</scp> -lactide)–poly(ε-caprolactone) diblock copolymers with different block length ratios. RSC Advances, 2017, 7, 22515-22523.	3.6	36
26	Structural changes and crystallization kinetics of polylactide under CO ₂ investigated using high-pressure Fourier transform infrared spectroscopy. Polymer International, 2015, 64, 1762-1769.	3.1	35
27	Flexible TPU/MWCNTs/BN composites for frequency-selective electromagnetic shielding and enhanced thermal conductivity. Composites Communications, 2021, 28, 100953.	6.3	35
28	Preparation of Porous Biodegradable Polymer and Its Nanocomposites by Supercritical CO ₂ Foaming for Tissue Engineering. Journal of Nanomaterials, 2012, 2012, 1-12.	2.7	34
29	Solvent Free Generation of Open and Skinless Foam in Poly(<scp>l</scp> -lactic) Tj ETQq1 1 0.784314 rgBT /O Engineering Chemistry Research, 2012, 51, 6722-6730.	verlock 10 ⁻ 3.7	If 50 347 To 34
30	Strategy to Enhance Conductivity of Polystyrene/Graphene Composite Foams via Supercritical Carbon Dioxide Foaming Process. Journal of Supercritical Fluids, 2018, 142, 52-63.	3.2	34
31	Effect of Macromolecular Chain Movement and the Interchain Interaction on Crystalline Nucleation and Spherulite Growth of Polylactic Acid under High-Pressure CO ₂ . Macromolecules, 2020, 53, 312-322.	4.8	33
32	Synthesis and characterization of a novel charring agent and its application in intumescent flame retardant polypropylene system. Journal of Applied Polymer Science, 2012, 123, 1636-1644.	2.6	32
33	Preparation of alumina-coated graphite for thermally conductive and electrically insulating epoxy composites. RSC Advances, 2015, 5, 55170-55178.	3.6	32
34	Preparation and properties of epoxy/BN highly thermal conductive composites reinforced with SiC whisker. Polymer Composites, 2016, 37, 2611-2621.	4.6	30
35	A novel route to the generation of porous scaffold based on the phase morphology control of co-continuous poly(Îμ-caprolactone)/polylactide blend in supercritical CO 2. Polymer, 2017, 118, 163-172.	3.8	30
36	Microcellular nanocomposites based on millable polyurethane and nano-silica by two-step curing and solid-state supercritical CO 2 foaming: Preparation, high-pressure viscoelasticity and mechanical properties. Journal of Supercritical Fluids, 2017, 130, 198-209.	3.2	30

Xia Liao

#	Article	IF	CITATIONS
37	Green Method to Widen the Foaming Processing Window of PLA by Introducing Stereocomplex Crystallites. Industrial & Engineering Chemistry Research, 2019, 58, 21466-21475.	3.7	30
38	Preparation and toughening performance investigation of epoxy resins containing carbon nanotubes modified with hyperbranched polyester. Polymer Bulletin, 2018, 75, 1013-1026.	3.3	29
39	Preparation of nanocellular foams from polycarbonate/poly(lactic acid) blend by using supercritical carbon dioxide. Journal of Polymer Research, 2013, 20, 1.	2.4	28

40 Influence of Surface-functionalized Graphene Oxide on the Cell Morphology of Poly(methyl) Tj ETQq0 0 0 rgBT /Overlock 10 Tf 50 622 T

41	Green and High-Expansion PLLA/PDLA Foams with Excellent Thermal Insulation and Enhanced Compressive Properties. Industrial & Engineering Chemistry Research, 2020, 59, 19244-19251.	3.7	27
42	Cellular structure design by controlling rheological property of silicone rubber in supercritical CO2. Journal of Supercritical Fluids, 2020, 164, 104913.	3.2	27
43	Thermoplastic polyurethane/polytetrafluoroethylene composite foams with enhanced mechanical properties and anti-shrinkage capability fabricated with supercritical carbon dioxide. Journal of Supercritical Fluids, 2020, 163, 104861.	3.2	25
44	Efficient electrical conductivity and electromagnetic interference shielding performance of double percolated polymer composite foams by phase coarsening in supercritical CO2. Composites Science and Technology, 2021, 213, 108895.	7.8	23
45	Nanocellular and needle-like structures in poly(<scp>l</scp> -lactic acid) using spherulite templates and supercritical carbon dioxide. RSC Advances, 2015, 5, 36320-36324.	3.6	22
46	Investigation on cure kinetics of epoxy resin containing carbon nanotubes modified with hyper-branched polyester. RSC Advances, 2018, 8, 29830-29839.	3.6	22
47	Reinforcement of Mechanical Properties of Silicone Rubber Foam by Functionalized Graphene Using Supercritical CO ₂ Foaming Technology. Industrial & Engineering Chemistry Research, 2020, 59, 22132-22143.	3.7	22
48	Novel electric conductive polylactide/carbon nanotubes foams prepared by supercritical CO2. Progress in Natural Science: Materials International, 2013, 23, 395-401.	4.4	21
49	Concentric ring-banded spherulites of six-arm star-shaped poly(ε-caprolactone) via subcritical CO2. RSC Advances, 2014, 4, 10144.	3.6	21
50	Realizing simultaneous toughening and reinforcement in polypropylene blends via solid die-drawing. Polymer, 2019, 161, 109-121.	3.8	20
51	Unusual hierarchical structures of micro-injection molded isotactic polypropylene in presence of an in situ microfibrillar network and a β-nucleating agent. RSC Advances, 2015, 5, 43571-43580.	3.6	19
52	Poly(methyl methacrylate) nanocomposites based on graphene oxide: a comparative investigation of the effects of surface chemistry on properties and foaming behavior. Polymer International, 2016, 65, 1195-1203.	3.1	19
53	Study on the creep behavior of polypropylene. Polymer Engineering and Science, 2009, 49, 1375-1382.	3.1	18
54	Effective in situ polyamide 6 microfibrils in isotactic polypropylene under microinjection molding: significant improvement of mechanical performance. Journal of Materials Science, 2016, 51, 10386-10399.	3.7	18

Χια Liao

#	Article	IF	CITATIONS
55	Effects of Process Temperatures on the Flow-Induced Crystallization of Isotactic Polypropylene/Poly(ethylene terephthalate) Blends in Microinjection Molding. Industrial & Engineering Chemistry Research, 2017, 56, 9467-9477.	3.7	18
56	Heat insulating PLA/HNTs foams with enhanced compression performance fabricated by supercritical carbon dioxide. Journal of Supercritical Fluids, 2021, 177, 105344.	3.2	18
57	A Green and Structure-Controlled Approach to the Generation of Silicone Rubber Foams by Means of Carbon Dioxide. Frontiers in Forests and Global Change, 2016, 35, 19-32.	1.1	17
58	The distinctive nucleation of polystyrene composites with differently shaped carbonâ€based nanoparticles as nucleating agent in the supercritical CO ₂ foaming process. Polymer International, 2018, 67, 1488-1501.	3.1	17
59	Influence of surface modified graphene oxide on the mechanical performance and curing kinetics of epoxy resin. Polymers for Advanced Technologies, 2020, 31, 1865-1874.	3.2	17
60	Effect of <i>in situ</i> poly(ethylene terephthalate) (PET) microfibrils on the morphological structure and crystallization behavior of isotactic polypropylene (iPP) under an intensive shear rate. Polymers for Advanced Technologies, 2015, 26, 1275-1284.	3.2	16
61	Effect of structure regulation of hyper-branched polyester modified carbon nanotubes on toughening performance of epoxy/carbon nanotube nanocomposites. RSC Advances, 2019, 9, 12864-12876.	3.6	16
62	Microstructure studies of isotactic polypropylene under natural weathering by positron annihilation lifetime spectroscopy. Journal of Polymer Research, 2015, 22, 1.	2.4	12
63	Effect of confinement on glass dynamics andÂfree volume in immiscible polystyrene/highâ€density polyethylene blends. Polymer International, 2015, 64, 892-899.	3.1	12
64	Morphology evolution and crystalline structure of controlledâ€rheology polypropylene in microâ€injection molding. Polymers for Advanced Technologies, 2016, 27, 494-503.	3.2	12
65	Effect of nanoparticles on the morphology and properties of PET/PP <i>in situ</i> microfibrillar reinforced composites. Polymer Composites, 2017, 38, 2718-2726.	4.6	12
66	The rheological property and foam morphology of linear polypropylene and long chain branching polypropylene. Journal Wuhan University of Technology, Materials Science Edition, 2013, 28, 798-803.	1.0	11
67	Creep-resistant behavior of beta-polypropylene with different crystalline morphologies. RSC Advances, 2016, 6, 30986-30997.	3.6	11
68	Fabrication of lightweight flexible thermoplastic polyurethane/multiwalled carbon nanotubes composite foams for adjustable frequency-selective electromagnetic interference shielding by supercritical carbon dioxide. Journal of Supercritical Fluids, 2022, 188, 105675.	3.2	11
69	Morphology and crystallization behavior of PCL/SAN blends containing nanosilica with different surface properties. Journal of Applied Polymer Science, 2016, 133, .	2.6	10
70	Investigation of chemiâ€crystallization and free volume changes of highâ€density polyethylene weathered in a subtropical humid zone. Polymer International, 2016, 65, 1474-1481.	3.1	10
71	Structure evolution and orientation mechanism of isotactic polypropylene during the twoâ€stage solid die drawing process. Journal of Applied Polymer Science, 2018, 135, 46581.	2.6	10
72	Ultralow Dielectric Constant Polyarylene Ether Nitrile/Polyhedral Oligomeric Silsesquioxanes Foams with High Thermal Stabilities and Excellent Mechanical Properties Prepared by Supercritical CO ₂ . Advanced Engineering Materials, 2022, 24, 2100874.	3.5	10

Χια Γιαο

#	Article	IF	CITATIONS
73	New understanding of the hierarchical distribution of isotactic polypropylene blends formed by microinjection-molded poly(ethylene terephthalate) and β-nucleating agent. RSC Advances, 2015, 5, 61127-61136.	3.6	9
74	Synergistic effect of multiwalled carbon nanotubes and carbon black on rheological behaviors and electrical conductivity of hybrid polypropylene nanocomposites. Polymer Composites, 2018, 39, E723.	4.6	9
75	Role of dicumyl peroxide on the morphology and mechanical performance of polypropylene random copolymer in microinjection molding. Polymers for Advanced Technologies, 2018, 29, 171-181.	3.2	9
76	Design of lightweight silicone rubber foam for outstanding deformation recoverability based on supercritical CO2 foaming technology. Journal of Materials Science, 2022, 57, 2292-2304.	3.7	9
77	Effect of physical and chemical crosslinking structure on fatigue behavior of styrene butadiene elastomer. Journal of Applied Polymer Science, 2014, 131, .	2.6	8
78	New insight into the flocculation behavior of hydrophilic silica in styrene butadiene rubber composites. RSC Advances, 2015, 5, 91262-91272.	3.6	8
79	Effects of enhanced compatibility by transesterification on the cell morphology of poly(lactic acid)/ polycarbonate blends using supercritical carbon dioxide. Journal of Cellular Plastics, 2015, 51, 349-372.	2.4	8
80	The improved foaming behavior of PLA caused by the enhanced rheology properties and crystallization behavior via synergistic effect of carbon nanotubes and graphene. Journal of Applied Polymer Science, 2022, 139, 51874.	2.6	8
81	Generating porous polymer microspheres with cellular surface via a gas-diffusion confined scCO2 foaming technology to endow the super-hydrophobic coating with hierarchical roughness. Chemical Engineering Journal, 2022, 442, 136192.	12.7	8
82	Flow-induced Î ² -crystal of iPP in microinjection molding: effects of addition of UHMWPE and the processing parameters. Journal of Polymer Research, 2016, 23, 1.	2.4	7
83	Influences of Hyperbranched Polyester Modification on the Crystallization Kinetics of Isotactic Polypropylene/Graphene Oxide Composites. Polymers, 2019, 11, 433.	4.5	7
84	Cellular structure design by controlling the dissolution and diffusion behavior of gases in silicon rubber. Journal of Supercritical Fluids, 2022, 186, 105610.	3.2	7
85	Rheological behaviors and electrical conductivity of long-chain branched polypropylene/carbon black composites with different methods. Journal of Polymer Research, 2015, 22, 1.	2.4	6
86	Ring-banded spherulites of six-arm star-shaped poly(Îμ-caprolactone) with different arm length via CO2. Colloid and Polymer Science, 2015, 293, 2311-2319.	2.1	6
87	The dependence time of melting behavior on rheological aspects of disentangled polymer melt: a route to the heterogeneous melt. Journal of Polymer Research, 2015, 22, 1.	2.4	6
88	Disclosing the crystallization behavior and morphology of poly(ïµâ€caprolactone) within poly(ïµâ€caprolactone)/poly(<scp>l</scp> â€lactide) blends. Polymer International, 2018, 67, 566-576.	3.1	6
89	Effect of Molecular Chain Mobility Induced by High-Pressure CO ₂ on Crystallization Memory Behavior of Poly(<scp>d</scp> -lactic Acid). Crystal Growth and Design, 2021, 21, 7116-7127.	3.0	6
90	Nonisothermal and isothermal crystallization behavior of isotactic polypropylene/chemically reduced graphene papocomposites. Polymer Composites, 2017, 38, F342	4.6	5

Χια Liao

#	Article	IF	CITATIONS
91	Mechanism of Microstructural Change of High-Density Polyethylene Under Different Outdoor Climates in China. Journal of Polymers and the Environment, 2020, 28, 2616-2630.	5.0	5
92	Effective enhancement of the creep resistance in isotactic polypropylene by elevated concentrations of DMDBS. RSC Advances, 2016, 6, 84801-84809.	3.6	4
93	Thermal oxidative and ozone oxidative stabilization effect of hybridized functional graphene oxide in a silica-filled solution styrene butadiene elastomer. Physical Chemistry Chemical Physics, 2016, 18, 29423-29434.	2.8	4
94	The crystallization morphology and process of stereocomplex crystallites of polylactide under CO ₂ : the effect of H-bonding and chain diffusion. CrystEngComm, 2021, 23, 8601-8611.	2.6	4
95	Effect of combined fatigue and chemical aging conditions on the mechanical property, structure, and morphology of styrene–butadiene–styrene elastomer. Journal of Elastomers and Plastics, 2015, 47, 681-696.	1.5	3
96	Confined crystallization morphology of poly(ϵâ€caprolactone) block within poly(ϵâ€caprolactone)–poly(lâ€lactide) copolymers. Polymer International, 2019, 68, 1992-2003.	3.1	3
97	Influence of Surfactant Functional Groups on Morphology and Rheology of Polypropylene/Organoclay Nanocomposites. Journal of Macromolecular Science - Physics, 2015, 54, 329-347.	1.0	2
98	Structure and Properties of Poly(Oxypropylene) Diamine Intercalated Montmorillonite/Epoxy Composites. Journal of Macromolecular Science - Physics, 2019, 58, 877-889.	1.0	2
99	Investigation on the crystallization behavior and detail spherulitic morphology of two crystal forms of thermoplastic polyurethanes. Journal of Polymer Research, 2022, 29, .	2.4	0